

Measurements of the Growth of the Ice Budget in a Persisting Contrail¹

R. G. KNOLLENBERG

Dept. of the Geophysical Sciences, The University of Chicago 60637
(Manuscript received 30 December 1971, in revised form 10 July 1972)

ABSTRACT

An experiment was conducted with the NCAR Sabreliner to measure the ice water content (IWC) and the total ice budget within its contrail. Particle size distributions were measured with an optical-array particle size spectrometer. The experiment was performed in a region of the atmosphere void of natural ice crystals (cirrus) but estimated to be above ice saturation and favorable to ice crystal growth.

The IWC measured was found to be in excess of 0.1 gm m^{-3} near the contrail axis with average values of a few hundredths of a gram throughout the contrail. The measured water mass within the contrail was found to be four orders of magnitude greater than that computed as a combustion product. Average crystal sizes of nearly 0.5 mm allow for a transfer of moisture at generation level to much lower levels before re-evaporation. Because of the magnitude of the measured effect and its believed frequent occurrence, the overall effect of sub-tropopause jet traffic is likely to lower the water abundance at the most traveled levels.

The total number of ice crystals produced is similar to the number of droplets expected in the initial liquid water contrail. All ice crystals appear to be produced through the freezing of droplets.

The rate of diffusional spreading of the contrail corresponds to an eddy diffusivity of $1.5 \times 10^6 \text{ cm}^2 \text{ sec}^{-1}$. No turbulence was detected and the diffusion appears isotropic after the rapid dissipation of the initial vortically organized turbulent wake.

1. Introduction

It is often observed that contrails spread considerably beyond the initial width defined by the outward extension of the wing-tip vortices. Under favorable conditions, a lateral spread of kilometers is observed with presumably comparable vertical spreading. If sufficient air carrier traffic exists, an entire overcast of contrail cirrus may develop and persist for hours with rapid growth in the ice budget of individual contrails.

One typically finds contrails growing (contrail growth hereafter meaning an increase in the ice budget) 100–200 mi ahead of an approaching winter cyclone. The author made some rough optical depth measurements on isolated contrails from the ground during February 1971 preceding a winter snow storm. Using the sun as a source, an average optical depth of 0.1 was found for a contrail which had developed a lateral spread of 15° (approximately 2.5 km wide at estimated altitude). With any reasonable particle size (e.g., 10μ) one estimates a total amount of ice along the flight path orders of magnitude greater than that exhausted from an aircraft. Since trails of particles were observed streaming from these contrails, the average particle size was more likely larger than 100μ .

That ice crystals in contrails would grow was recognized by Appleman (1953) and others in early contrail studies. However, outside of the isolated crystal col-

lections by Weickmann (1945), the growth of large crystals in contrails and the development of large ice water contents can only be inferred from their visual appearance and optical measurements. The growth of contrails with large ice crystals and ice water contents orders of magnitude greater than that due to the water supplied by aircraft exhausts presents an alternate thesis in the current arguments over whether jet air carrier traffic increases or decreases water abundance at sub-tropopause levels. At these altitudes, fairly large ice crystals will fall thousands of feet before evaporating. Given sufficient probability for conditions of such growth, the overall effect of sub-tropopause jet traffic may in fact be to lower the water abundance in this region of the atmosphere through the precipitation of existing moisture to much lower levels. The possibility of such a result provided the thrust for direct measurements of the ice budget in growing contrails. The experiment simply involves the use of a jet aircraft with controlled engine performance factors to produce a contrail under conditions favorable to its growth and then make repetitive sampling penetrations orthogonal to the flight track. The primary instrument used to measure the ice budget was an optical-array particle size spectrometer (Knollenberg, 1970). A brief description of this particle spectrometer and the experimental design follows.

2. Instrumentation and experimental design

The optical-array spectrometer used in this study is shown in Fig. 1. This particular unit uses a photodiode

¹ This research was sponsored by the National Aeronautics and Space Administration under Grant NGR 14-001-148 and the National Science Foundation through the National Center for Atmospheric Research.



FIG. 1. Optical-array particle size spectrometer installed on NCAR Sabreliner.

array instead of the fiber optics array common to earlier systems. It is a prototype of a NASA system being designed for a future Venus entry probe. A 1-mW He-Ne laser is used in the system to illuminate the crystals. The crystals are imaged with a single objective lens providing a $1.33\times$ magnification. The photodiodes were masked on $200\ \mu$ centers resulting in $150\ \mu$ resolution. The system uses 16 photodiodes resulting in 14 size channels ranging from $75\ \mu$ to 2.175 mm in $150\ \mu$ size intervals. Coupled with the external probe is a memory and display system providing a real-time graphical CRT display of the measured particle size distributions and reading out a complete distribution eight times a second. The spectrometer operated continuously during the 12 hr of operations in contrails and natural cirrus at altitudes over 36,000 ft and temperatures below -55°C .

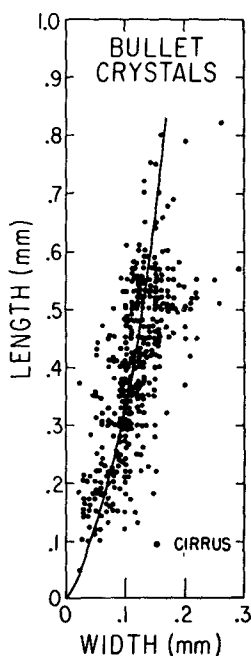


FIG. 2. Bullet crystal aspect ratios from measurements in natural cirrus (after Heymsfield and Knollenberg, 1972).

The spectrometer was mounted on top of the Sabreliner fuselage behind the pilot's canopy (see Fig. 1) and while not an ideal location for cloud droplets, proved to be quite satisfactory for the larger sizes encountered in this study. Besides the state parameter measurements, a Doppler navigational system provided wind and logistics information useful for penetration profile reconstruction.

The ice crystal distributions measured by the spectrometer were corrected for particle orientation under the assumption that the particles were bullets with their major crystal axis in the horizontal plane. Our studies in natural cirrus indicate that the majority of all cirrus crystals are bullets with over 95% bullets in the generating regions. The remainder are primarily columns which have nearly identical masses to bullets of equal length. The probe, looking vertically at the crystals randomly oriented in a horizontal plane, gives a random cosine response to the crystal length. A transform to correct for this effect has been used routinely on natural cirrus crystals and found to give distributions in excellent agreement with collections from replicated samples. Since the cosine is nearly unity for one-third of all orientations and the small axis of the crystals is at least 20% of the crystal length (5:1 aspect ratio) even for the largest crystals observed (1.5 mm), the total effect of transforming the distribution is not nearly as large as one might first suspect. The aspect ratios and densities for bullets used in transforming the raw data and in computing crystal mass are shown in Figs. 2 and 3.

The lower size limit of $75\ \mu$ does not permit particle detection until the crystals have had time to grow. The loss of measurement of particles $<75\ \mu$ does not allow measuring all of the ice water content and hence our measurements tend to underestimate the total. However, crystals $>75\ \mu$ will fall out of the contrail, and in regions below the level of contrail generation or in any region where the crystals have had time to grow to larger sizes, we find that we sample nearly all of the ice water content.

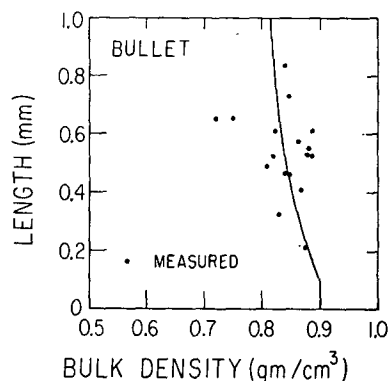


FIG. 3. Bullet crystal densities from measurements in natural cirrus (after Heymsfield and Knollenberg, 1972).

The Sabreliner aircraft has twin jet engines each capable of consuming 1200 lb hr^{-1} of fuel. In the contrail experiments we used an engine setting which gave a total fuel consumption rate of 1500 lb hr^{-1} and an indicated airspeed of 180 kt. Partial approach flaps were applied to keep the aircraft level at this slow airspeed. At 30,000 ft the aircraft trues out at 280–300 kt or nearly 150 m sec^{-1} . The fuel consumption rate and airspeed convert to 1.26 gm of fuel burned per meter of flight path. Using a conversion factor of 1.37 gm of water per gm of fuel (JP-4), this converts to $1.73 \text{ gm H}_2\text{O}$ per meter of flight path deposited through exhaust. In comparisons of contrail growth, we will integrate the ice water contents over the contrail cross section to give mass per meter of flight path.

3. Experimental results and analysis

During the 10 days allotted for the research program, conditions were favorable for contrail growth only on 16 and 19 September. Missions were flown on both of these days.

On 16 September, a massive upslope “summer” snow storm was developing along the front range. The early afternoon was characterized by a thickening lower deck, drizzle and lowering temperatures. An extensive band of contrail cirrus had already developed by the time we arrived at altitude (1400 MDT). While growth in the ice budget of our own contrail was observed and we were able to sample it, a detailed analysis of the data was not attempted because of possible confusion with the complex pattern of neighboring contrail cirrus and the rapidly changing meteorological situation. Suffice to say, the contrail cirrus deck thickened to the west and gradually merged with the tops of the thickening lower deck as the afternoon progressed.

On 19 September natural cirrus was visible at 30,000 ft over the mountains of northern Colorado and southern Wyoming. This region is not on major airways and contrails were not evident. By 1200 MDT we were in the region of natural cirrus which was developing between 25,000 and 30,000 ft. We found a few isolated cirrus uncinus about 50 n mi south of Laramie, Wyo., and after several sampling runs, observed our contrail from a prior run persisting over several kilometers of flight path. A photograph of the contrail is shown in Fig. 4 taken 12 min after generation. The initial time of contrail generation was 1208:28 as determined from Doppler derived air-track plots.

The meteorological conditions at the time of contrail generation are shown in Fig. 5. Also shown are the boundary conditions (critical temperature required to produce water saturation) given by Appleman (1953) for contrail formation. The contrail was generated in a region of negative wind shear at -38.2°C at an altitude of 29,500 ft (326 mb).

On approaching the contrail, precipitation trails were just emerging and an increase in the ice budget

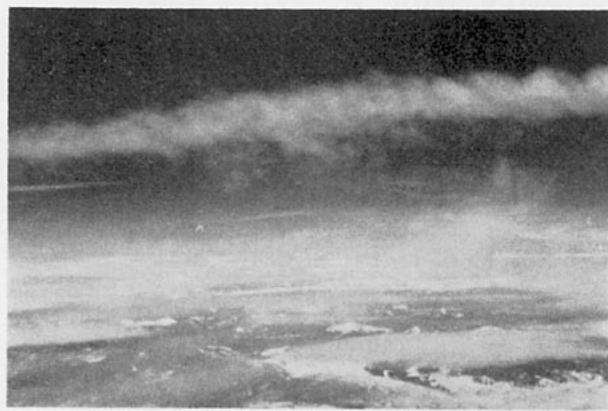


FIG. 4. Photograph of Sabreliner contrail taken 12 min after generation (photograph contrast enhanced).

was apparent. Because the particle size in the contrail was estimated to be small, the pass was made just at the point of emergence of the trails from the contrail. This initial pass through the contrail at 1222 revealed an IWC of $\sim 0.05 \text{ gm m}^{-3}$ in the most concentrated region (see Fig. 6). Upon emergence from the contrail, the downwind side was seen to possess a ragged, highly structured appearance in contrast with the uniform upwind side which appeared as a core region. (Visual sightings of such structures in contrails are quite common when viewed from the ground.) During the course of the experimental measurements, the contrail core finally broke into patches similar in appearance to a line of cirrus uncinus with the original contrail core appearing as the generating heads (Fig. 7). The entire contrail and the generated virga were visible for almost an hour.

Data from the contrail core were analyzed in detail and its structure became evident on examining multi-level passes. Two cross sections constructed from these

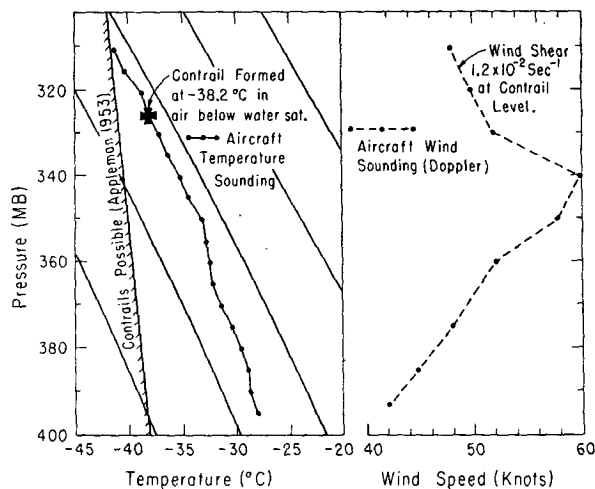


FIG. 5. Meteorological conditions on 19 September 1971, measured during contrail experiment. Contrail formed at a temperature several degrees above Appleman's (1953) critical value.

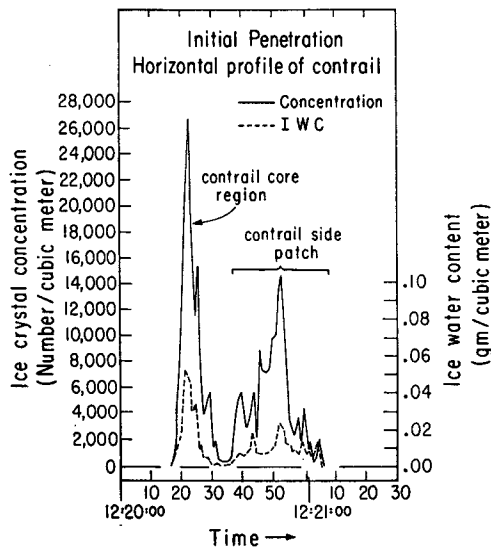


FIG. 6. Concentration and ice water content horizontal profiles in contrail 18 min after generation.

data are given in Figs. 8 and 9. The upper passes in these cross sections were within 100 m of the top of the contrail core and the estimated IWC isopleths should be reasonably good. The lower levels are less certain.

The size distributions in regions of high IWC are similar in appearance to those in low IWC, the change in IWC following the change in concentration very closely and not strongly influenced by crystal size (see Figs. 8 and 9). Many of the distributions in these passes were nearly closed, indicating that large numbers of smaller crystals were not present. Other distributions are characterized by exponentially increasing concentration with decreasing size and presumably significant concentrations below the $75\ \mu$ limit of detection. The lack of any major difference in the crystal size distributions indicates that growth conditions are similar throughout the contrail environment. However, it became apparent after several subsequent penetrations



FIG. 7. Photograph of contrail regions which appear similar to cirrus uncinus (photograph contrast enhanced).

that there is a limited supply of ice crystals, and as growth proceeds the larger crystals fall out leaving smaller crystals to grow until the entire supply is exhausted. Both cross sections show the highest IWC in the region of the lowest passes which is probably the result of continued growth during fallout. The final pass in the same region as the upper pass in cross section A, but 12 min later (1247) revealed only a few crystals remaining at this level. The entire region rapidly decayed and completely disappeared by 1300.

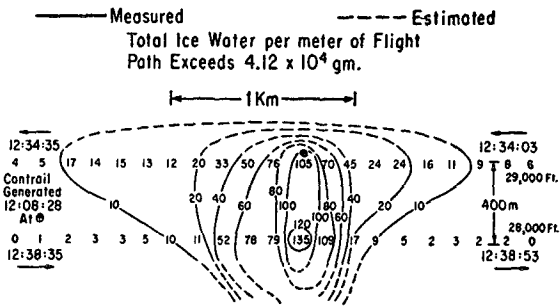
Since the contrail core was a fairly continuous segment, computations of total ice per meter of flight path should be suitable for comparison with the exhausted water from the aircraft. Only the region between the passes was integrated. The values computed were $4.12 \times 10^4\ \text{gm m}^{-1}$ and $2.07 \times 10^4\ \text{gm m}^{-1}$ for cross sections A and B. There are at least four orders of magnitude more ice present in the contrail core than the Sabreliner originally exhausted! Furthermore, these values are underestimates for the following reasons:

- 1) The IWC above and below the pass levels wasn't added to the total ice m^{-1} .
- 2) The IWC in satellite patches such as that in Fig. 6 obviously arose from the contrail and once added would increase the ice m^{-1} .
- 3) During the course of the experiment (45 min) a continuous flux of crystals was falling out to lower levels and evaporating.
- 4) The spectrometer measured no IWC from crystals smaller than $75\ \mu$.

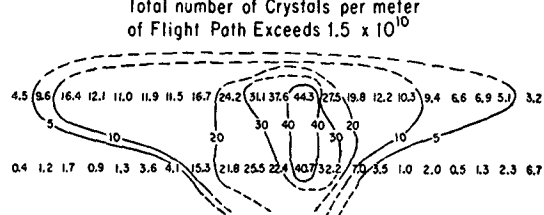
1), 2) and 4) above are probably insufficient to raise the ice m^{-1} more than a factor of 2. However, 3) may be of considerable importance. The average terminal velocity computed for the largest crystals observed in the initial pass was over $2\ \text{m sec}^{-1}$. In the 1800 sec of observations, the core was seen to actually increase its IWC. If one assumes merely a steady state in the number of larger crystals (which was observed), they would have to be replenished nine times in the 29,000–28,000 ft level during the time of observation. Much of the IWC is in these larger sizes, and the actual amount of ice formed may be much more than the values determined. One can usually point to wind shear as a mechanism to provide virgin air to falling crystals (e.g., in cirrus uncinus) to increase growth. However, this particular contrail was oriented parallel to the wind direction with negligible lateral shear. Shear was thus of little importance to crystal growth or contrail spreading.

The horizontal profile of the concentration data in these cross sections is similar to the uniform distributions computed and observed for line source turbulent diffusion processes. No vortical structure is evident and, indeed if present, it would not be apparent in this data because of the separation of the particle trajectories from the vortical streamlines. In addition, the

Ice Water Content ($\text{gm} \times 10^{-3} / \text{cubic meter}$)



Ice Crystal Concentrations (number $\times 10^3 / \text{cubic meter}$)



Ice Crystal Size Spectra

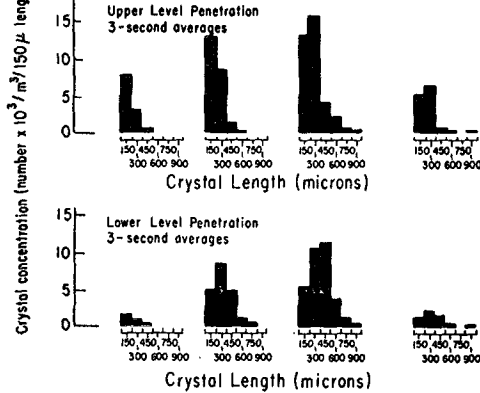


Fig. 8. Ice crystal concentrations, ice water content, and ice crystal size spectra cross sections for region A of contrail.

Sabreliner engines are aft mounted on the narrow part of the fuselage and the two individual contrails rapidly merge resembling those from an aircraft with a single centrally placed engine. According to Scorer and Davenport (1970), the trail from such an aircraft would simply descend vertically and not circulate with the vortex pair. While a contrail obviously initially descends, the measurements indicate that early in its lifetime the contrail spread to higher levels. This may be due to mixing by the vortex pair, but the vertical growth is as easily explained as a response to buoyancy due to latent heat release. It is unlikely that the latent heat released during the initial highly supersaturated growth phase can be dissipated as fast as it is released. Thus, a positively buoyant situation initially arises. Overall, the contrail did lower during the measurement period due to ice crystal fallout.

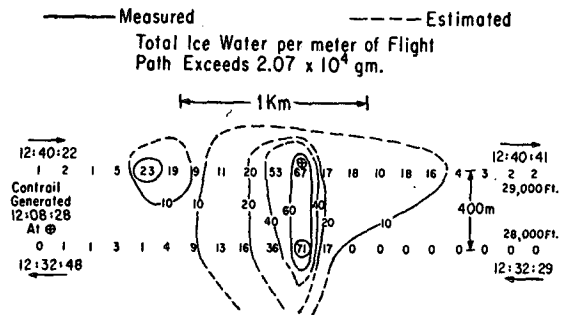
The fact that the Gaussian concentration profile was quite profound suggested a possible simple mathematical treatment of the data. The spreading of a contaminant (or ice crystals) from an infinite line source is given by

$$\bar{c} = \frac{Q}{4\pi Kt} \exp[-(X^2 + Z^2)/(4Kt)], \quad (1)$$

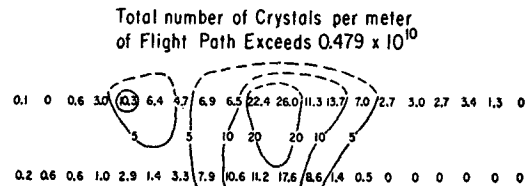
where \bar{c} is the average concentration, Q the total initial source generation, K the turbulent diffusion coefficient, t time, X horizontal distance, and Z vertical distance, and all units are cgs.

By determining the total number of crystals initially formed and using the cross-section data, one can compute the average turbulent diffusion coefficient for the

Ice Water Content ($\text{gm} \times 10^{-3} / \text{cubic meter}$)



Ice Crystal Concentrations (number $\times 10^3 / \text{cubic meter}$)



Ice Crystal Size Spectra

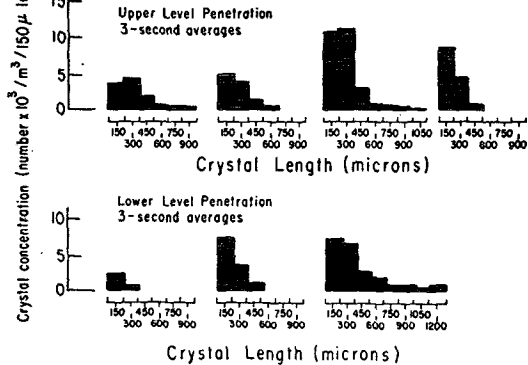


Fig. 9. Ice crystal concentration, ice water content, and ice crystal size spectra cross sections for region B of contrail.

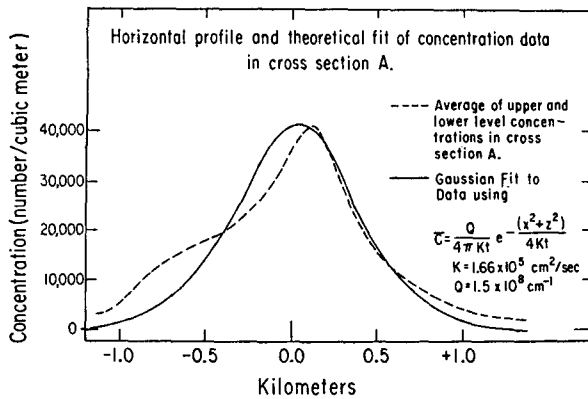


FIG. 10. Comparison of measured horizontal concentration profile ($Z=0$) with theoretical solution for an infinitely long line source of $1.5 \times 10^8 \text{ cm}^{-1}$.

time between measurement and initial formation. The value of Q used is simply the instantaneous value measured since accounting for those too small to be detected and those fallen out is unnecessary in the application of (1). The best fit of the data in cross section A with Eq. (1) results with a value of $K = 1.66 \times 10^5$. The fit can only be observed in the horizontal, since due to fallout, the vertical comparison would be very difficult. The comparison is shown in Fig. 10. The value of K computed for cross section B is $1.19 \times 10^5 \text{ cm}^2 \text{ sec}^{-1}$. These turbulent diffusion coefficients are average values for the approximately 1800 sec between generation and measurement of the contrail. The values, while above average, are not unreasonable for the ambient atmosphere at these levels.

It should be pointed out that the majority of the lateral spreading was measured after the dissipation of the vortices. The diffusion appears isotropic and while the origin of the turbulent energy is partially from the vortices, the rate of spreading was observed to be nearly constant and suggestive of ambient atmospheric characteristics. The effect of wind shear upon lateral spreading can be neglected due to the alignment of the contrail with wind direction.

One may also compute the eddy dissipation rate using

$$\epsilon = K\beta^2,$$

where ϵ is the eddy dissipation rate and β the wind shear. The measured wind shear at these levels was about $1.2 \times 10^{-2} \text{ sec}^{-1}$. Thus, for the cross section A

$$\epsilon = 1.66 \times 10^{-5} \times (1.2 \times 10^{-2})^2 = 23.9 \text{ cm}^2 \text{ sec}^{-3},$$

and for cross section B

$$\epsilon = 16.1 \text{ cm}^2 \text{ sec}^{-3}.$$

Both values of ϵ correspond to conditions of weak CAT (see Atlas *et al.*, 1966). Indeed, all penetrations of the contrail region could be characterized as quite smooth.

The computed value of Q also provides clues as to

microphysical processes early in the life of the contrail. The values of approximately 10^{10} crystals per meter of flight path are quite high when one considers that the Sabreliner aircraft exhausts less than 10^6 cm^3 every meter of flight path. Approximately 10^4 ice nuclei cm^{-3} must be present in the exhaust. This value is only about an order of magnitude less than the number of condensation nuclei one would anticipate in the exhaust. One must therefore conclude that ice nucleation must proceed rapidly (as it should at -38.2°C), affecting a good percentage of the initial droplets nearly simultaneously. If nucleation proceeded slowly the ice crystals initially formed would rapidly cause evaporation of unnucleated water droplets and much fewer ice crystals would be produced. At temperatures 10°C warmer one would expect greatly reduced numbers of active ice nuclei. It may not be apparent but the formation of an order-of-magnitude fewer ice crystals would result in the glaciation of a contrail with one-tenth of the optical depth of the one in this study. Such a glaciated trail may not be visible from the ground. The reader should bear in mind that it is the optical depth or amount of scattering cross section that is relevant to a contrail's visibility. The use of some value of LWC or IWC as a visibility criterion for contrails is void of interpretation in the absence of particle size information. The early condensed liquid phase of a *highly visible* contrail may have droplets only a few tenths of a micron in diameter and a few thousandths of a gram IWC while the *less visible* glaciated state has ice crystals a few hundred microns in length and a tenth of a gram IWC.

4. Discussion of contrail formation, persistence and growth

It is the current thinking among many cloud physicists that ice nucleation rarely occurs in the atmosphere without prior condensation of water. If the same applies to aircraft exhaust products the formation of contrails will occur only if the vapor trail reaches water saturation. However, water saturation may not occur in the vapor trail even though the air was saturated prior to the aircraft's penetration and the effect may result in evaporation of existing clouds (distrails). The aircraft exhaust always heats the moisture enriched air and saturation is only reached after mixing with the environment. Once a contrail has formed, it can persist as a water trail if the ambient air is saturated with respect to water, persist as an ice trail if rapidly glaciated and the ambient air is saturated with respect to ice, or it may grow in total ice mass if glaciated and the ambient air is above ice saturation. Thus, as defined here, contrail *persistence* is limited to describing a static budget in the water substance while *growth* requires an increase in this budget.

Appleman (1953) was the first to develop criteria for contrail formation over a wide range of altitudes,

temperatures and humidities. An essential result of his study was the prediction of whether water saturation is reached following the mixing of the exhausted heat and water vapor with the ambient air. His treatment describes the change in mixing ratio (decrease) in the aircraft wake as being proportional to the change in wake temperature (decrease) with the proportionality constant fuel-dependent only. With any given fuel (or proportionality constant) there results a *critical* temperature for each altitude above which contrail formation is impossible. In order that the contrail be visible a temperature as much as several degrees below the critical temperature is generally required.

In this experiment, as shown in Fig. 5, we actually observed the contrail to form and grow at a temperature several degrees above the critical temperature as defined by Appleman (1953) or the laboratory contrail studies of Pilie and Jiusto (1958). According to the analysis of Appleman (1953), at this altitude a temperature of below -40°C and ambient water saturation would be required for a contrail to form. The absence of nearby cirrus makes ambient water saturation unlikely, although supersaturation with respect to ice is quite probable.

One possible explanation is a positive error in our temperature measuring equipment. However, another rather simple explanation of this observation is apparent after examining the heat budget of a contrail. It should be remarked that not all of the energy from fuel combustion appears as heat immediately, as assumed in all prior work. The aircraft also imparts a considerable amount of mechanical energy to the atmosphere in performing the work necessary for flight. Inevitably, this mechanical energy also appears as heat but not before condensation occurs in certain cases, and as will be seen below, after condensation occurs the condensed particles may rapidly radiate away the total heat produced through combustion allowing such "impossible" contrails to persist and grow. One may further point to the perturbations in temperature and pressure brought about by the trailing vortex pair and unequal mixing of heat and water vapor as sufficient to cause transient regions for condensation.

a. Influence of radiative divergence

Once condensation has produced a visible contrail of some optical depth, radiation acting on the particles provides another mechanism for heat exchange. Kuhn's (1970) measurements show a 12% reduction in solar insolation by such a contrail sheet. The effects of this solar depletion are important to the heat budget at the earth's surface but have little effect on the heat budget of contrails. The effect on the contrail heat budget is apparent from measurements of radiative divergence. During the same day Kuhn (1970) made the measurements reported, he was also able to measure the radiative divergence of the contrail left by the NASA

Convair 990 six minutes after generation. He found an average cooling rate of $20.9^{\circ}\text{C day}^{-1}$ over the entire contrail layer and $30^{\circ}\text{C day}^{-1}$ at the top of the contrail layer.² The contrail was estimated to be 300 m deep and 400 m wide at the time measurements were made. The measured cooling rate of $20.9^{\circ}\text{C day}^{-1}$ corresponds to a heat loss of 3×10^9 cal hr^{-1} per kilometer of flight path! An aircraft burning 3600 lb of fuel an hour and flying at 500 kt exhausts only 3×10^7 calories of heat per kilometer of flight path. Thus, in only seconds radiational losses dissipated the same amount of heat added through exhaust emission. It should be clear that a depth of 300 m is not required to reach the same conclusion, only that the total optical cross section remain the same. By comparison, the author has computed cooling rates of $5^{\circ}\text{C hr}^{-1}$ in the tops of natural cirrus using observed particle size information and an Elsasser flux computation. Similar values in contrails should at least be possible since the optical cross section is usually greater.

Radiational cooling of the contrail layer also results in added condensation and increased particle growth. Under conditions characterized by radiational cooling ice crystals radiate more energy than they correspondingly receive and the ice crystals' temperature is suppressed. The magnitude of the effect is proportional to the crystal size. If ambient conditions are between ice and water saturation, the heat of sublimation exchanged during crystal growth can be at least partially radiated, increasing the particle growth rate over conditions of radiative equilibrium. Growth of large crystals at subsaturated conditions would also be predicted. The suggested growth at subsaturated conditions results from theoretical studies and from radiative divergence measurements, but it is difficult to verify from aircraft humidity measurements because of the poor response of hygrometers at cirrus altitudes. However, Gotaas and Bensen (1965) reported that ice fogs persisted at *measured* conditions subsaturated with respect to ice. The magnitude of their measured subsaturation was re-examined by Bowling *et al.* (1971) and found to be too large, although subsaturation is still suggested.

Radiational cooling characterizes cirrus and contrails at subtropause levels at mid-latitudes from October to May; however, at higher levels and in the summer months, radiational heating dominates. The principal factor that determines the radiative divergence is the window radiation between 6.5 and 14μ . In the summer months the window is "hot" and the radiation absorbed by a particle exceeds that it emits (radiational heating). At stratospheric levels, particle temperatures are lower and the decreased emitted radiation must be compared with about the same window radiation as at lower levels (again radiational heating is most likely). On the other hand, the outgoing window radiation is always

² Unpublished data furnished to the author through personal communication with P. M. Kuhn.

reduced by intervening cloud layers, and their effect is always to increase the likelihood of radiational cooling at higher cloud levels.

From the above discussion it is obvious that radiational cooling aids contrail persistence and growth. In most cases, this adds to the potential for growth which simply results from ambient supersaturation with respect to ice. However, in certain cases contrails can also grow when the ambient air is initially subsaturated with respect to ice.

5. Conclusions

The ice budget as determined by particle size distributions suggests that these contrails are not unlike natural cirrus. The generating region is initially brought to water saturation with subsequent condensation and a fairly rapid freezing. The concentrations and IWC were similar to those found in nearby natural cirrus. Observations indicate that all of the ice crystals form within the initial condensation trail and once the supply is exhausted through virga, no further ice crystals appear. Crystal multiplication processes are not indicated. The effect of the contrail is thus to provide an initial surplus of water sufficient to reach water saturation. Once the ice phase is present, the vapor density rapidly suppresses toward ice saturation and in the presence of radiative divergence, below ice saturation. Additional nucleation of ice crystals is therefore prohibited.

The results of this experiment are relevant to several questions of an environmental nature. There has been increasing concern over the amount of cirrus triggered through contrail formation. These results would not, however, suggest that increased air carrier traffic could increase the water vapor at subtropopause levels, a theme that is currently fashionable. On the contrary, the development of large numbers of precipitation size ice crystals in contrails results in precipitation and an ultimate exchange of water vapor to lower levels. Given reasonable frequency of contrail growth occurrence, the net effect of air carrier traffic may likely, in fact, be to lower the water abundance at the levels of most frequent air travel. This writer is currently of that opinion. During the month of October, contrail spreading and persistence was observed on 13 out of 31 days in Chi-

cago. It should not, however, be denied that at the same time contrail growth and persistence increases the optical cross section at sub-tropopause levels, thus more strongly affecting the radiation balance.

Of a cloud physics nature is the entire question of the effect of contrail cirrus as an added source region for ice crystals and perhaps preactivated nuclei. Contrails form huge numbers of ice crystals in an otherwise clear atmosphere. Their effect on lower cloud forms may provide a boost to the ice mechanism. The added impact of this ice crystal source region to that provided by natural cirrus is purely conjecture. Certainly it is an area where research must be applied to obtain defensible conclusions.

Acknowledgments. The author would like to thank the NCAR Research Aviation Facility and the Computing Facility for their support during this research effort. In particular, I would like to cite Mr. Edward Brown for his aid during the flight program and Mr. Dean Frey for data processing assistance. Also, Dr. Peter Kuhn of NOAA unselfishly furnished radiational cooling data from his contrail measurements.

REFERENCES

- Appleman, H., 1953: The formation of exhaust condensation trails by jet aircraft. *Bull. Amer. Meteor. Soc.*, **31**, 14-20.
- Atlas, D., K. R. Hardy and K. Naito, 1966: Optimizing the radar detection of clear air turbulence. *J. Appl. Meteor.*, **5**, 450-460.
- Bowling, S. A., C. S. Bensen and W. B. Murcay, 1971: Quasi-equilibrium temperature differences between radiating ice crystals and the surrounding air. *J. Appl. Meteor.*, **10**, 991-993.
- Gotaas, G., and C. S. Bensen, 1965: The effect of suspended ice crystals on radiative cooling. *J. Appl. Meteor.*, **4**, 446-453.
- Heymsfield, A. J., and R. G. Knollenberg, 1972: Properties of cirrus generating cells. *J. Atmos. Sci.*, **29**, 1358-1366.
- Knollenberg, R. G., 1970: The optical array: An alternative to extinction or scattering for airborne particle size determination. *J. Appl. Meteor.*, **9**, 86-103.
- Kuhn, P. M., 1970: Airborne observations of contrail effects on the thermal radiation budget. *J. Atmos. Sci.*, **27**, 937-942.
- Pilie, R. J., and J. E. Jiusto, 1958: A laboratory study of contrails. *J. Meteor.*, **15**, 149-154.
- Scorer, R. S. and L. J. Davenport, 1970: Contrails and aircraft downwash. *J. Fluid Mech.*, **43**, 451-464.
- Weickmann, H., 1945: Formen und Bildung atmosphärischer Eiskristalle. *Beitr. Phys. Atmos.*, **28**, 12-52.